Supplementary Material

Development of a multistep reaction cascade for the synthesis of a sacubitril precursor in continuous flow

Katharina Hiebler, Carina Dertnig, Sebastian Soritz, Manuel C. Maier, Theresa R. Hörmann, Bianca Grabner, Heidrun Gruber-Woelfler

Institute of Process and Particle Engineering, Graz University of Technology, Inffeldgasse 13/III, 8010 Graz, Austria

Corresponding author: Heidrun Gruber-Woelfler, woelfler@tugraz.at, +43 316 873 30406

Content

1.1 $^{1}H/^{13}C$-NMR spectra of 13, 14 and 16

NMR-measurements were performed using a Bruker Avance III 300 MHz spectrometer (^{1}H: 300 MHz, ^{13}C: 75 MHz). The chemical shift (δ [ppm]) was reported relatively to the used solvent $CDCl_3$ (7.26, s). For designation of multiplicities of observed coupling patterns, following abbreviations were used: s (singlet), d (doublet), dd (duplicated doublet), t (triplet), q (quartet), m (multiplet), bs (broad signal).

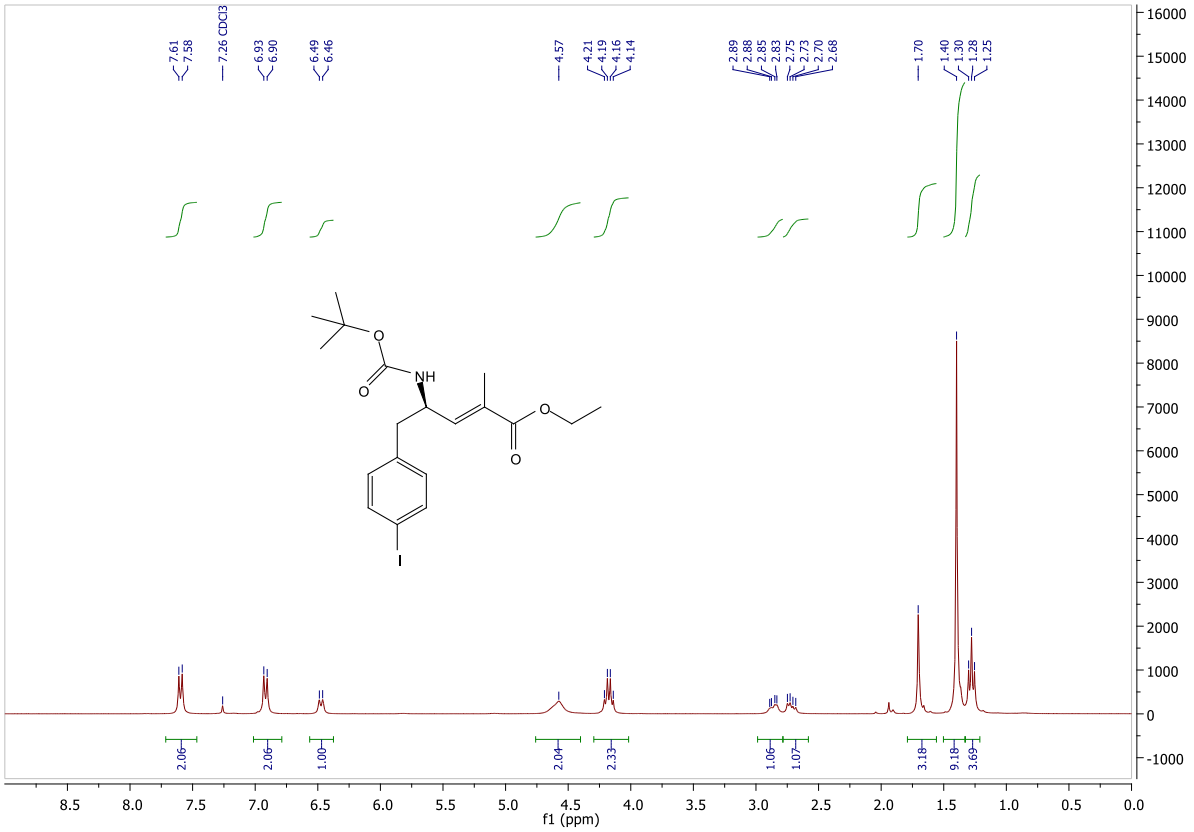

Figure 1: ^{1}H-NMR of **13** in $CDCl_3$.

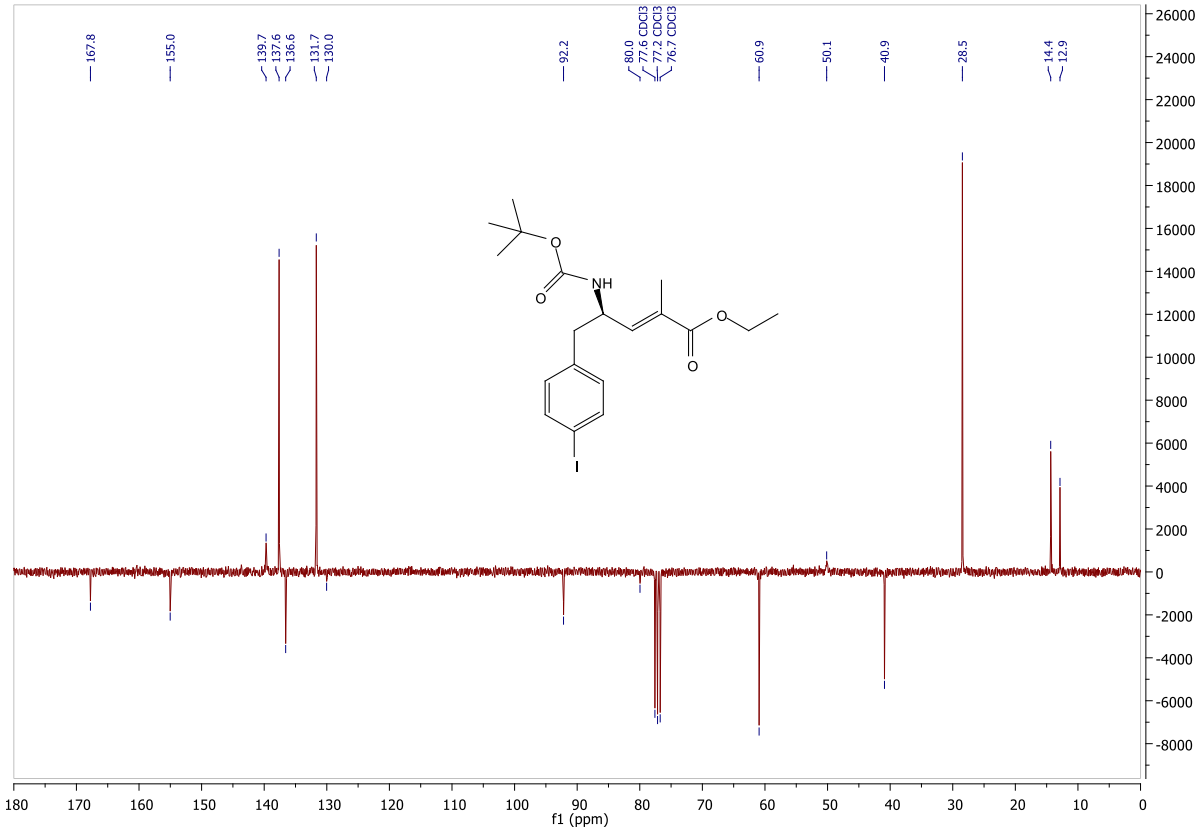

Figure 2: ^{13}C-NMR (APT) of **13** in $CDCl_3$.

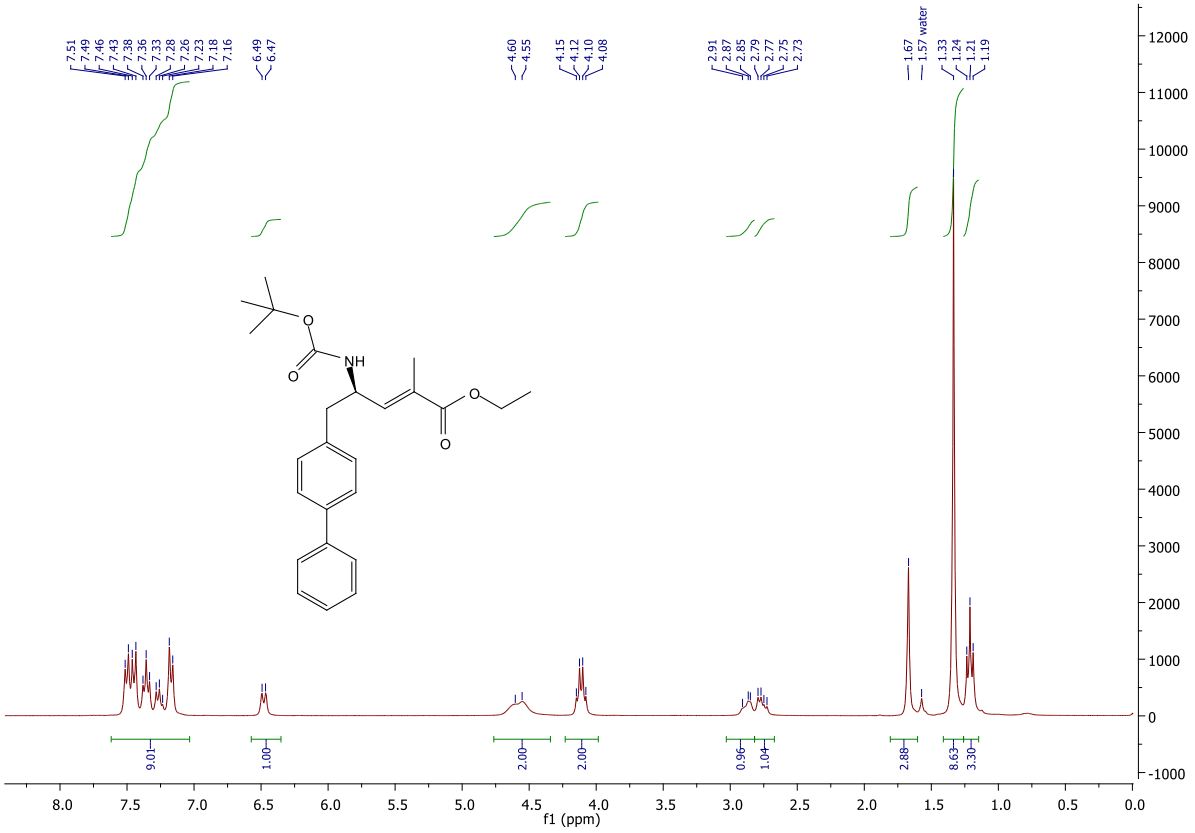

Figure 3: ^{1}H-NMR of **14** in $CDCl_3$.

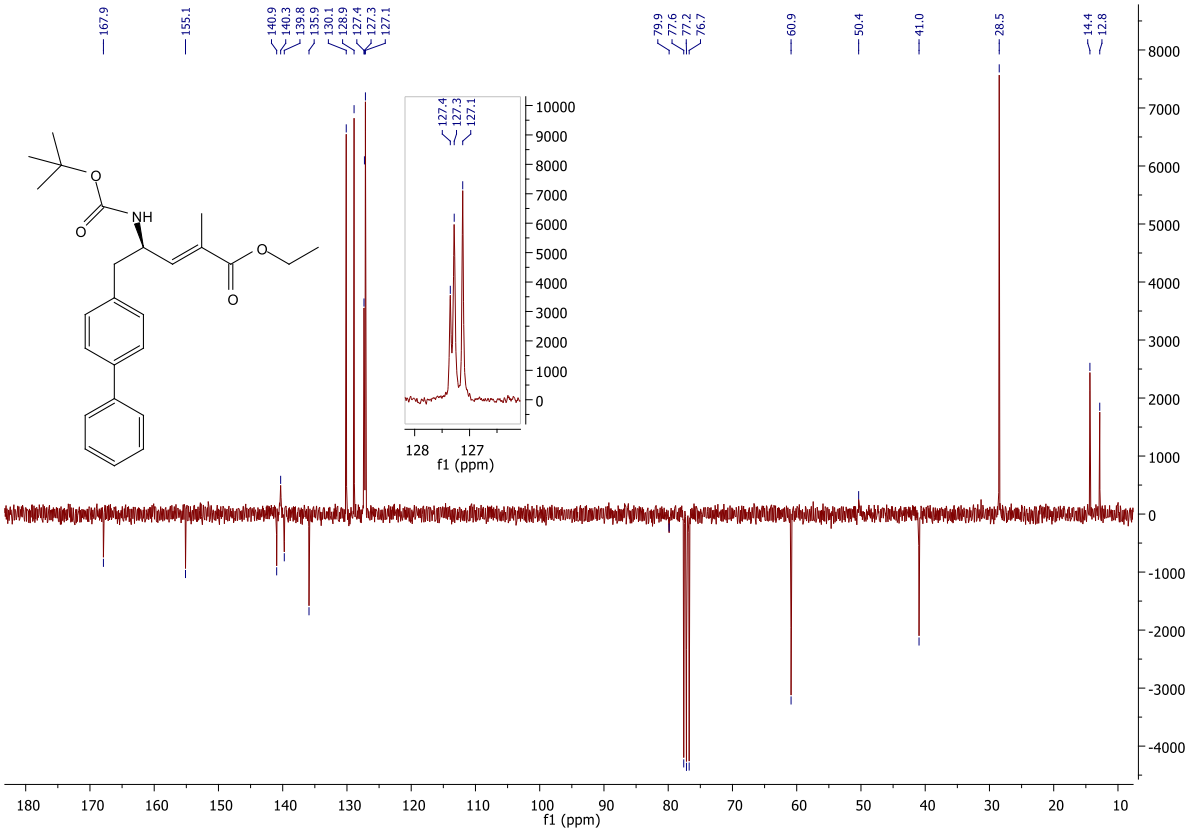

Figure 4: ^{13}C-NMR (APT) of **14** in $CDCl_3$.

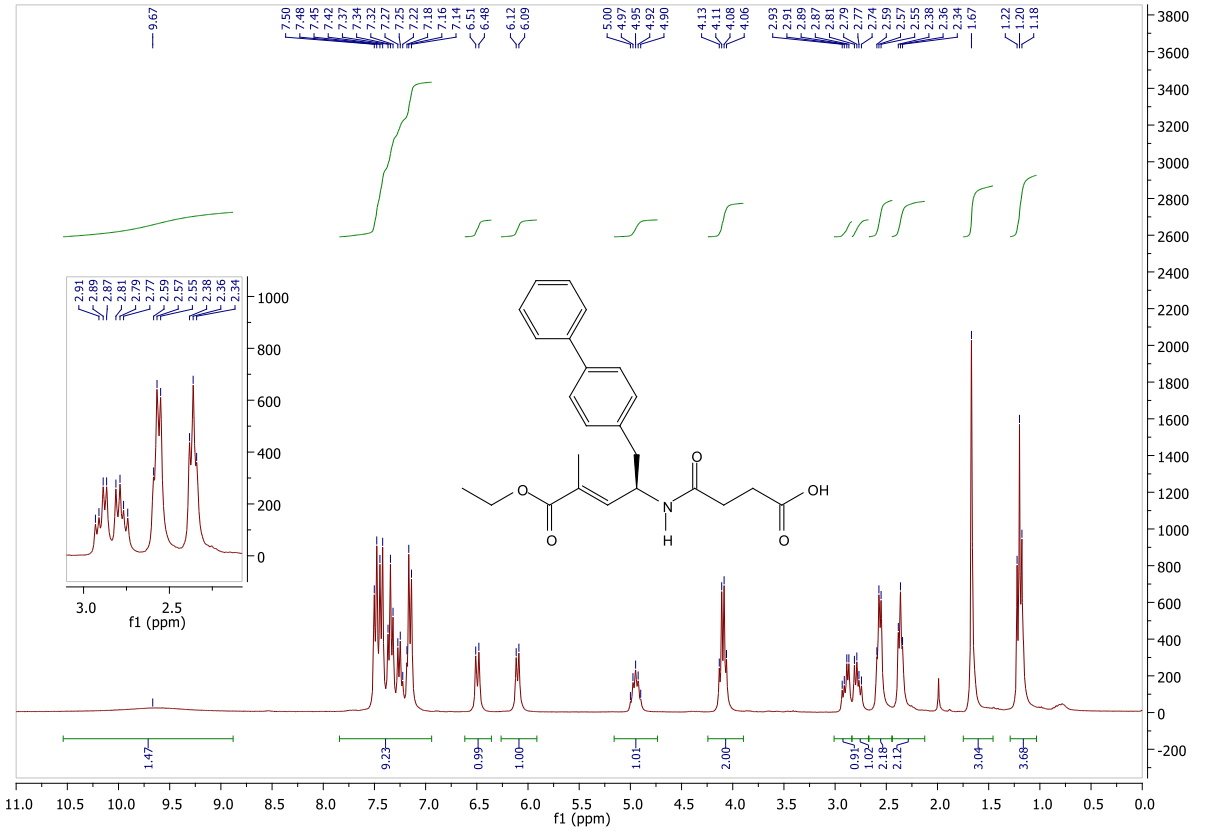

Figure 5: ^{1}H-NMR of **16** in $CDCl_3$.

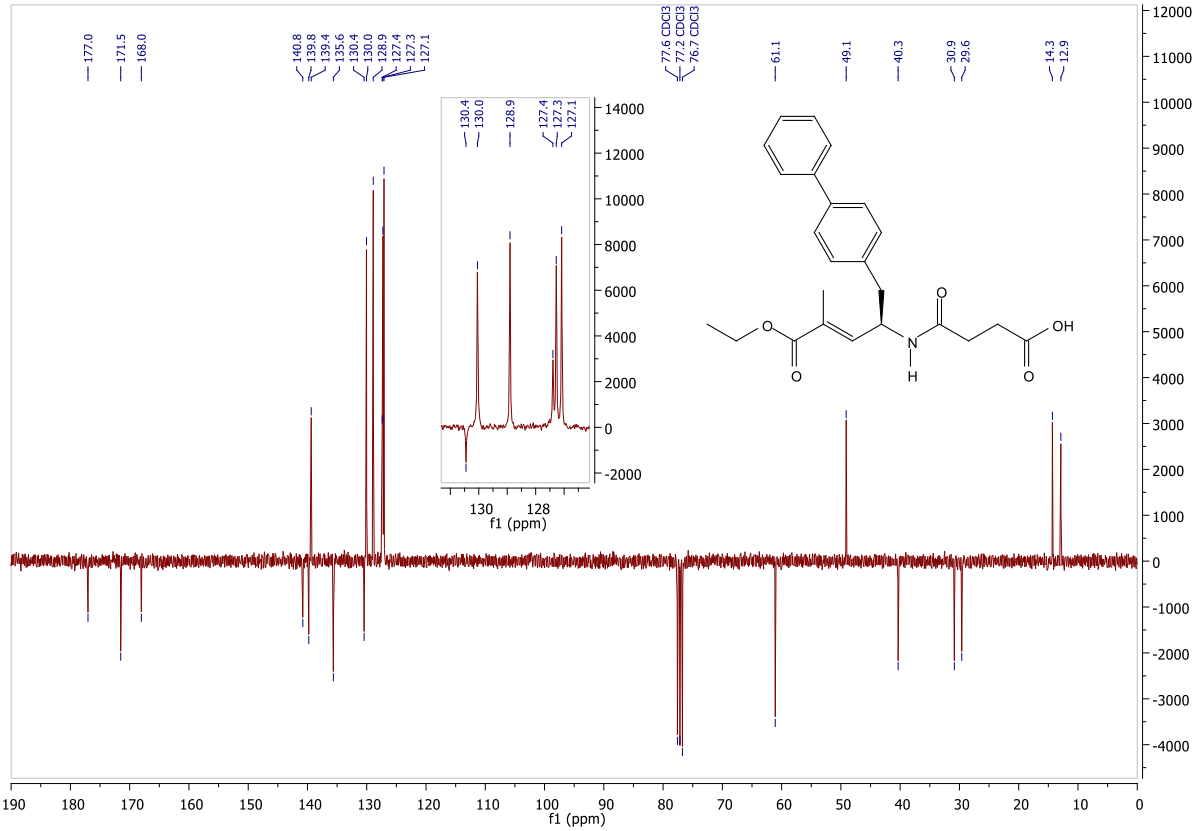

Figure 6: ^{13}C-NMR (APT) of **16** in $CDCl_3$.

1.2 High performance liquid chromatography (HPLC)

1.2.1 Reaction monitoring

The reaction progress of the flow reactions was monitored by High Performance Liquid Chromatography. Aliquots drawn from the flow reaction outlet were quenched with the respective sample diluent and analyzed using an Agilent 1100 series HPLC system equipped with an online degasser, quaternary pump, autosampler, thermostated column compartment and UV-visible diode array detector. As mobile phases, MeOH (solvent A) and aq. phosphoric acid (H_2O:H_3PO_4=300:1 v/v; solvent B) were used. Compounds were separated using a ThermoFischer Scientific Accucore™ C18 reversed phase column (50 x 4.6 mm; 2.6 µm) at 25 °C with a flow rate of 1 mL/min and detected by UV-absorption over the run time of 5 min. Used isocratic elution methods are summarized in Table 1.

Table 1: HPLC methods (% A = % MeOH, % B = % H_2O:H_3PO_4=300:1 v/v) for monitoring of the reaction progress.

Method	% A (v/v)	% B (v/v)	Sample diluent	Flow [mL/min]
A	55	45	MeOH:H_2O=55:45	1
B	75	25	MeOH:H_2O=75:25	1

The retention times (t_R) of the analyzed compounds are apparent from Table 2.

Table 2: Retention times of compounds separated by HPLC.

Compound	Method	λ [nm]	t_R [min]
Anisole	A	270	1.6
	B	270	0.8
13	B	237	2.2
14	B	237	3.2
16	B	237	1.1
17	A	210	3.6
18	A	210	0.5
19	A	210	0.8

1.2.2 Determination of enantiomeric purity

Enantiomeric excess of compounds **13**, **14** and **16** was determined using an Agilent 1100 Series HPLC system equipped with a temperature controlled oven and a UV detector. As mobile phase, n-hexane:ethanol (+ trifluoroacetic acid as mobile phase modifier if necessary) was used and samples were prepared in ethanol. A Daicel Chiralpak® OJ-H column (250 x 4.6 mm, 5 µm) was employed for separation of the chiral compounds over the run time of 20 min. Utilized isocratic elution methods are summarized in Table 3. The chromatographic elution order of the stereoisomers was determined by comparison with synthesized (*S*)- and (*R*)-reference compounds.

Table 3: HPLC methods (% A= % n-heptane, % B= % ethanol, % C= % trifluoroacetic acid) for determination of the enantiomeric excess.

Method	% A (v/v)	% B (v/v)	% C (v/v)	T [°C]	Flow [mL/min]	Time [min]
A	80	20	0	40	1.5	20
B	80	20	0.01	40	1.5	20

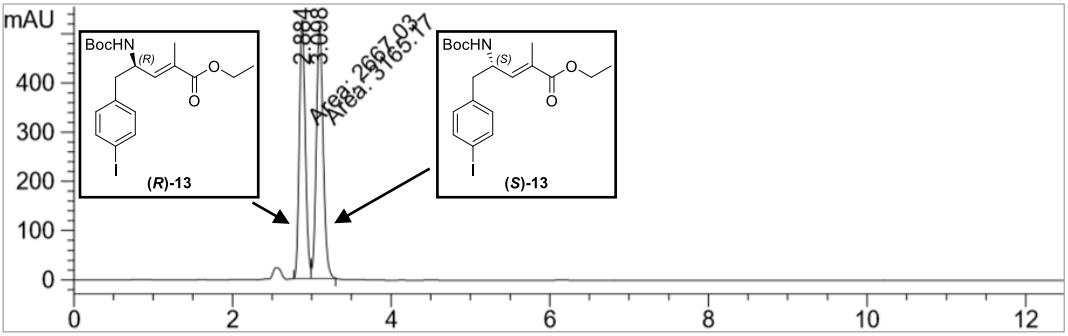

Figure 7: Chiral separation of **(*R*)-** and **(*S*)-13** by HPLC (λ= 237 nm).

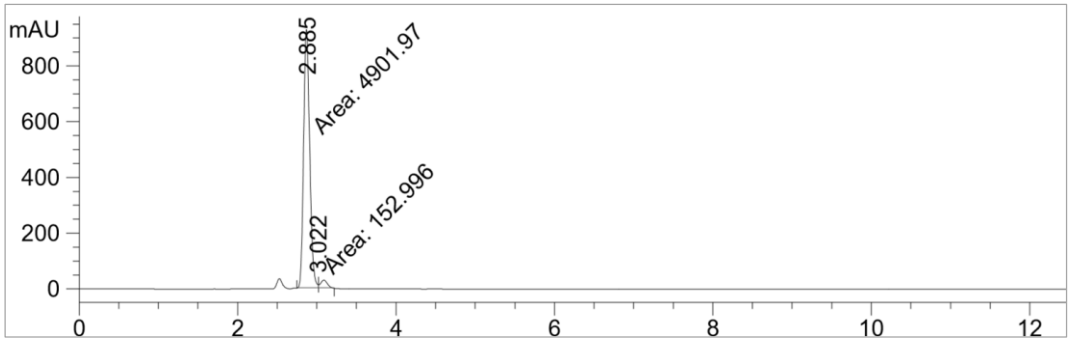

Figure 8: Determination of enantiomeric excess of compound **13** synthesized in batch (λ= 237 nm).

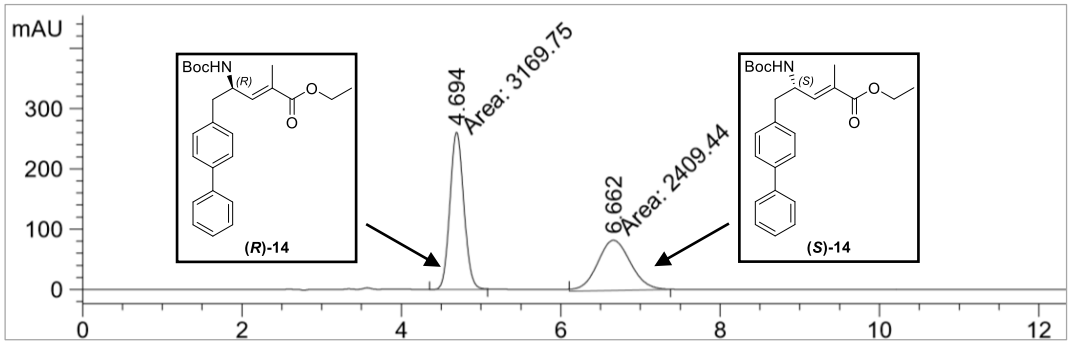

Figure 9: Chiral separation of **(*R*)-** and **(*S*)-14** by HPLC (λ= 270 nm).

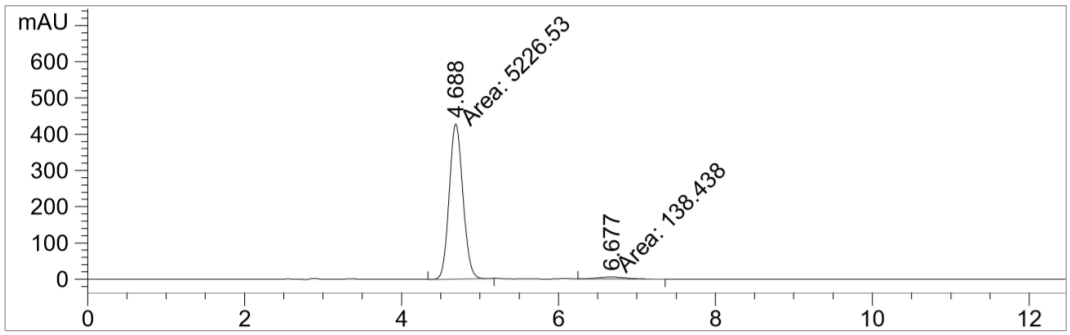

Figure 10: Determination of enantiomeric excess of compound **14** synthesized in flow (λ= 270 nm).

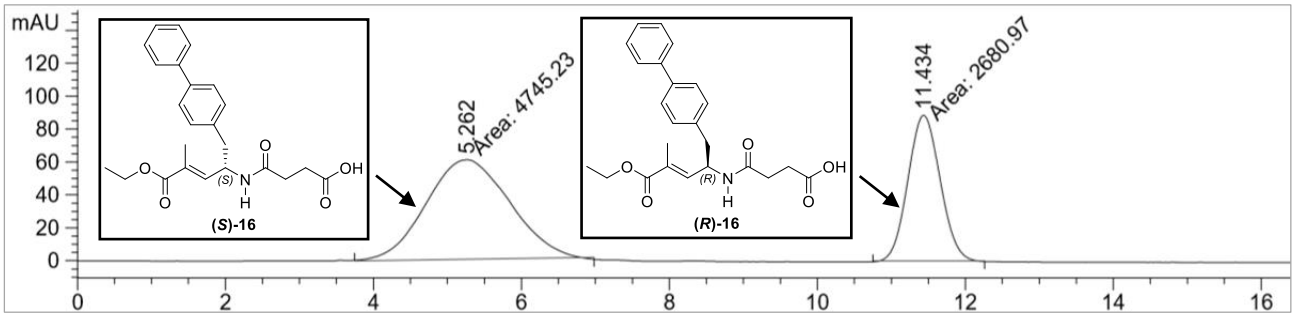

Figure 11: Chiral separation of **(*R*)-** and **(*S*)-16** by HPLC (λ= 270 nm).

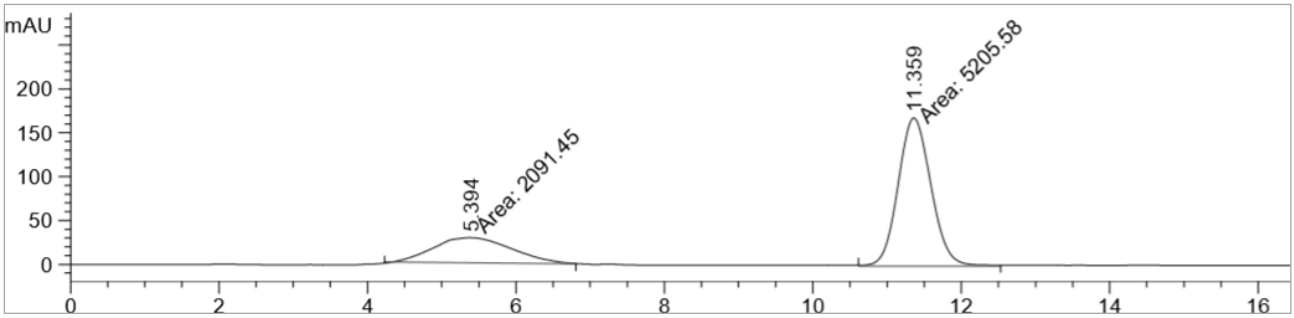

Figure 12: Determination of enantiomeric excess of compound **16** synthesized in flow (λ= 270 nm).

Table 4: Retention times of compounds separated by chiral HPLC.

Compound	Method	λ [nm]	t_R [min]
(***R***)-**13**	A	237	2.9
(***S***)-**13**	A	237	3.1
(***R***)-**14**	A	270	4.7
(***S***)-**14**	A	270	6.7
(***R***)-**16**	B	270	11.4
(***S***)-**16**	B	270	5.3

1.3 Chemical syntheses of 13, 14, 16 and $Ce_{0.20}Sn_{0.79}Pd_{0.01}O_{2-\delta}$

1.3.1 Synthesis of ethyl-(*R*,*E*)-4-((*tert*-butoxycarbonyl)amino)-5-(4-iodophenyl)-2-methylpent-2-enoate 13

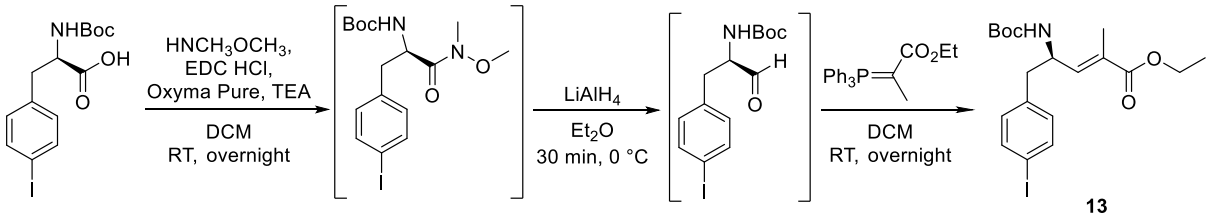

The reaction was performed based on a similar synthesis procedure described by Ksander et al. [1] under argon atmosphere using Schlenk technique. Boc-4-iodo-D-phenylalanine (2.92 g, 7.48 mmol, 1.15 mol eq.), *O*,*N*-dimethylhydroxylamine hydrochloride (0.63 g, 6.50 mmol), 1-ethyl-3-(3-dimethylaminopropyl)carbodiimide hydrochloride (2.85 g, 14.9 mmol, 2.29 mol eq.), ethyl(hydroxyimino)cyanoacetate (1.60 g, 11.3 mmol, 1.73 mol eq.) and triethylamine (1.24 mL, 8.91 mmol, 1.37 mol eq.) were dissolved in dichloromethane (25 mL) and the orange reaction solution was stirred overnight at room temperature. The solvent was carefully evaporated from the dark brown reaction mixture and the residue was diluted with ethyl acetate (50 mL). The organic phase was washed with sat. aq. $NaHCO_3$ (2 x 30 mL), 1 M HCl (2 x 30 mL) and brine (1 x 30 mL) successively and dried over Na_2SO_4. The solvent was removed under reduced pressure to yield crude *tert*-butyl-(*R*)-(3-(4-iodophenyl)-1-(methoxy(methyl)amino)-1-oxopropan-2-yl)carbamate as a brownish viscous oil, which was directly used in the next step without further purification.

Crude *tert*-butyl-(*R*)-(3-(4-iodophenyl)-1-(methoxy(methyl)amino)-1-oxopropan-2-yl)carbamate (6.50 mmol) was dissolved in dry diethyl ether (110 mL) and cooled to 0 °C. $LiAlH_4$ (1.0 M in diethyl ether, 13.0 mL, 13.0 mmol, 2.00 mol eq.) was added dropwise and the reaction mixture was kept stirring for 30 min at 0 °C. After quenching the reaction with cold 5% aq. $KHSO_4$ (44.3 mL, 16.3 mmol, 2.50 mol eq.), the reaction mixture was warmed to room temperature and washed with cold 1 M HCl (2 x 40 mL) and brine (2 x 40 mL, 1 x 20 mL) successively. The organic phase was dried over Na_2SO_4. The solvent was removed under reduced pressure to yield crude *tert*-butyl-(*R*)-(1-(4-iodophenyl)-3-oxopropan-2-yl)carbamate as a yellow solid, which was used in the next step without further purification.

Crude *tert*-butyl-(*R*)-(1-(4-iodophenyl)-3-oxopropan-2-yl)carbamate (6.50 mmol) and (carbethoxyethylidene)triphenylphosphorane (4.71 g, 13.0 mmol, 2.00 mol eq.) were dissolved in dichloromethane (110 mL) and the reaction mixture was stirred at room temperature overnight. Then, the solvent was removed under reduced pressure and crude **13** was purified by column chromatography (silica gel, toluene:ethyl acetate = 95:5) giving **13** (1.64 g, 3.58 mmol) as a white solid in 55% overall yield.

Thin layer chromatography (SiO_2): toluene:ethyl acetate = 95:5, R_f = 0.3

^{1}H-NMR (300 MHz, $CDCl_3$): δ_H [ppm]= 7.60 (d, *J*= 8.1 Hz, 2H, -C*H*Cl-), 6.92 (d, *J*= 8.1 Hz, 2H, -C*H*CHCl-), 6.47 (d, *J*= 7.8 Hz, 1H, -C*H*=C-), 4.76 – 4.40 (m, 2H, -C*H*N*H*-), 4.18 (q, *J*= 7.1 Hz, 2H, -CH_2CH$_3$-), 2.86 (dd, J_1= 12.6 Hz, J_2= 4.5 Hz, 1H, -C$_{ar}$CH_2-), 2.72 (dd, J_1= 13.4 Hz, J_2=6.7 Hz, 1H, -C$_{ar}$CH_2-), 1.70 (s, 3H, -CH=C(CH_3)-), 1.40 (s, 9H, -C(CH_3)$_3$), 1.28 (t, *J*= 7.1 Hz, 3H, -CH$_2$CH_3).

^{13}C-NMR (75 MHz, $CDCl_3$): δ_C [ppm]= 167.8 (-C*C*OO-), 155.0 (-N*C*OO-), 139.7 (-*C*H=C-), 137.6 (2C, -*C*HCl-), 136.6 (-*C*$_{ar}$CH$_2$-), 131.7 (2C, -*C*HCHI-), 130.0 (-CH=*C*-), 92.2 (-*C*I-), 80.0 (-*C*(CH$_3$)$_3$-), 60.9 (-*C*H$_2$CH$_3$), 50.1 (-*C*HNH-), 40.9 (-C$_{ar}$*C*H$_2$-), 28.5 (3C, -C(*C*H$_3$)$_3$), 14.4 (-CH$_2$*C*H$_3$), 12.9 (-CH=C(*C*H$_3$)-).

No NMR data of **13** were available in literature. However, ^{1}H- and ^{13}C-NMR data are in accordance with the corresponding literature data of a similar compound, where the iodo-substituent on the aromatic ring is replaced by a hydrogen atom [2].

HPLC/MS-ES (*m/z*) found 460.33, calcd for $[M+H]^+$ 460.32

1.3.2 Synthesis of ethyl-(*R*,*E*)-5-([1,1'-biphenyl]-4-yl)-4-((*tert*-butoxycarbonyl)amino)-2-methylpent-2-enoate 14

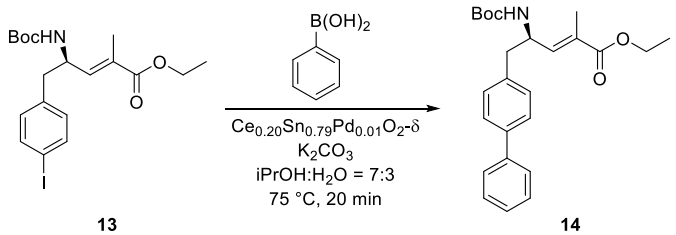

13 **14**

Compound **13** (300 mg, 0.65 mmol), phenylboronic acid (120 mg, 0.98 mmol, 1.50 mol eq.) and potassium carbonate (135 mg, 0.98 mmol, 1.50 mol eq.) were dissolved in 2-propanol:H_2O = 7:3 (v/v, 25 mL). The reaction mixture was stirred at 75 °C until all reactants were dissolved and Pd-catalyst $Ce_{0.20}Sn_{0.79}Pd_{0.01}O_{2-\delta}$ (94 mg, 1 mol%) was added. After 20 min, HPLC analysis showed completion of the reaction. The solvent was evaporated under reduced pressure, the residue was diluted with ethyl acetate (25 mL) and washed with H_2O (2 x 15 mL) as well as brine (1 x 15 mL). The organic phase was dried over Na_2SO_4 and the solvent was removed under reduced pressure. The crude product was purified by column chromatography (silica gel, PE:EtOAc = 85:15) to give **14** (165 mg, 0.40 mmol) as a white solid in 62% yield.

Thin layer chromatography (SiO_2): Petrol ether:ethyl acetate = 85:15, R_f = 0.7

^{1}H-NMR (300 MHz, $CDCl_3$): δ_H [ppm]= 7.62 – 6.99 (m, 9H, all -C*H*$_{ar}$-), 6.48 (d, *J*= 7.9 Hz, 1H, -C*H*=C-), 4.82 – 4.40 (m, 2H, -C*H*N*H*-), 4.11 (q, *J*= 7.0 Hz, 2H, -C*H*$_2$CH$_3$), 2.88 (dd, J_1= 12.8 Hz, J_2=5.0 Hz, 1H, -C*H*$_2$C$_{ar}$-), 2.76 (dd, J_1= 13.3 Hz, J_2= 6.7 Hz, 1H, -C*H*$_2$C$_{ar}$-), 1.67 (s, 3H, -CH=C(C*H*$_3$)-), 1.33 (s, 9H, -C(C*H*$_3$)$_3$), 1.21 (t, *J*= 7.1 Hz, 3H, -CH$_2$C*H*$_3$).

^{13}C-NMR (75 MHz, $CDCl_3$): δ_C [ppm]= 167.9 (-*C*OOCH$_2$CH$_3$), 155.1 (-*C*OOC(CH$_3$)$_3$), 140.9 (-CH$_2$Ph*C*$_{ar}$-), 140.3 (-*C*H=C-), 139.8 (-CH$_2$(CCHCH*C*)$_{ar}$-), 135.9 (-CH$_2$*C*$_{ar}$-), 130.1 (2C, -CH$_2$(*C*CH)$_{ar}$-), 128.9 (2C, -CH$_2$Ph(CCH*C*H)$_{ar}$-), 127.4 (-CH$_2$Ph(CCHCH*C*H)$_{ar}$-), 127.3 (2C, -CH$_2$Ph(*C*CH)$_{ar}$-), 127.1 (2C, -CH$_2$(CCH*C*H)$_{ar}$-), 79.9 (-*C*(CH$_3$)$_3$), 60.9 (-*C*H$_2$CH$_3$), 50.4 (-*C*HNH-), 41.0 (-*C*H$_2$C$_{ar}$-), 28.5 (3C, -C(*C*H$_3$)$_3$), 14.4 (-CH$_2$*C*H$_3$), 12.8 (-CH=C(*C*H$_3$)-).

^{1}H-data were in accordance with the literature values [1]. No ^{13}C-NMR data of **14** were available in literature. However, the ^{13}C-NMR were in accordance with the corresponding literature values (C_q=CH signal too weak to be visible) of a similar compound bearing a phenyl instead of a biphenyl substituent [2].

HPLC/MS-ES (*m/z*) found 410.45, calcd for $[M+H]^+$ 410.53

1.3.3 Synthesis of (*R*,*E*)-4-((1-([1,1'-biphenyl]-4-yl)-5-ethoxy-4-methyl-5-oxopent-3-en-2-yl)amino)-4-oxobutanoic acid 16

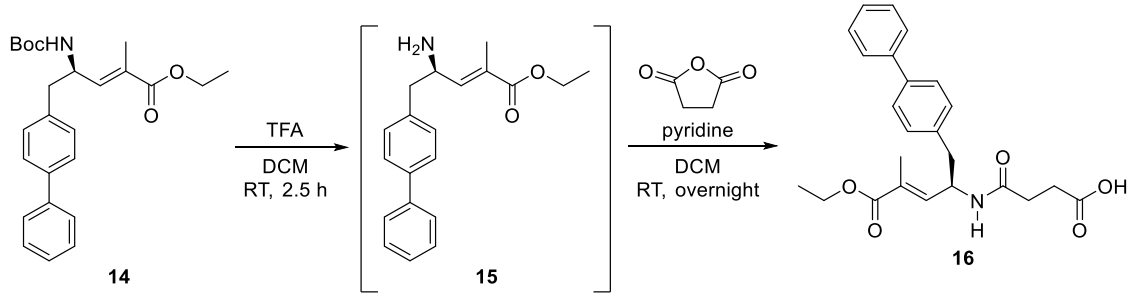

Compound **14** (100 mg, 0.25 mmol) was dissolved in dichloromethane (1.5 mL) and trifluoroacetic acid (1.50 mL, 19.6 mmol, 80.0 mol eq.) was added slowly to the reaction mixture, which was kept stirring at room temperature for 2.5 h. The solvent was removed under reduced pressure and the residual oil was diluted with ethyl acetate (20 mL) and washed with sat. aq. Na_2CO_3 (2 x 10 mL) as well as brine (1 x 10 mL) successively. The organic phase was dried over Na_2SO_4 and the solvent was removed under reduced pressure to yield **15** (75.8 mg) as a yellow oil. The crude product was used in the next step without further purification.

Based on a similar synthesis procedure performed by Ksander et al. [1], crude **15** (0.25 mmol) was dissolved in dichloromethane (1.5 mL) and pyridine (1.5 mL). Succinic anhydride (37.2 mg, 0.37 mmol, 1.52 mol eq.) was added. After stirring the reaction mixture overnight at room temperature, the solvent was removed by rotary evaporation. The residue was diluted with ethyl acetate (20 mL), washed with 1 M HCl (3 x 10 mL) and brine (1 x 10 mL) successively and the organic phase was dried over Na_2SO_4. The solvent was removed under reduced pressure and crude **16** was purified by column chromatography (silica gel, ethyl acetate + 0.5 % acetic acid) giving **16** (70.2 mg, 0.17 mmol) as a yellowish oil in 70% overall yield.

Thin layer chromatography (SiO_2): ethyl acetate + 0.5 % acetic acid, R_f = 0.6

^{1}H-NMR (300 MHz, $CDCl_3$): δ_H [ppm]= 9.67 (bs, 1H, -O*H*), 7.85 – 6.91 (m, 9H, -C_{ar}*H*-), 6.50 (d, *J*= 9.2 Hz, 1H, -C*H*=C-), 6.10 (d, *J*= 7.9 Hz, 1H, -N*H*), 4.95 (dt, J_1= 14.9 Hz, J_2= 7.4 Hz, 1H, -C*H*NH-), 4.10 (q, *J*= 7.0 Hz, 2H, -C$H_2$$CH_3$-), 2.90 (dd, J_1= 13.5 Hz, J_2= 6.1 Hz, 1H, -C_{ar}CH_2-), 2.78 (dd, J_1= 13.5 Hz, J_2= 7.2 Hz, 1H, -C_{ar}CH_2-), 2.57 (t, *J*= 6.0 Hz, 2H, -CH_2COOH), 2.36 (t, *J*= 6.2 Hz, 2H, -C$H_2$$CH_2$COOH), 1.67 (s, 3H, -CH=C(CH_3)-), 1.20 (t, *J*= 7.1 Hz, 3H, -CH_2CH_3).

^{13}C-NMR (75 MHz, $CDCl_3$): δ_C [ppm]= 177.0 (-*C*OOH), 171.5 (-*C*ONH-), 168.0 (-*C*OOCH_2-), 140.8 (-CH_2PhC_{ar}-), 139.8 (-CH_2(CCHCH*C*)$_{ar}$-), 139.4 (-*C*H=C-), 135.6 (-$CH_2$$C_{ar}$-), 130.4 (-CH=*C*-), 130.0 (2C, -CH_2(C*C*H)$_{ar}$-), 128.9 (2C, -CH_2Ph(CCH*C*H)$_{ar}$-), 127.4 (-CH_2Ph(CCHCH*C*H)$_{ar}$-), 127.3 (2C, -CH_2Ph(C*C*H)$_{ar}$-), 127.1 (2C, -CH_2(CCH*C*H)$_{ar}$-), 61.1 (-*C*$H_2$$CH_3$), 49.1 (-*C*HNH-), 40.3 (-C_{ar}*C*H_2-), 30.9 (-*C*H_2COOH), 29.6 (-*C*$H_2$$CH_2$COOH), 14.3 (-$CH_2$*C*$H_3$), 12.9 (-CH=C(*C*$H_3$)-).

No NMR data of compound **16** were available in literature. However, the ^{1}H- and ^{13}C-NMR values were comparable with the corresponding literature data of sacubitril [3] except from the signals corresponding to the C-C double bond.

HPLC/MS-ES (*m/z*) found 410.46, calcd for $[M+H]^+$ 410.48

1.3.4 Synthesis of the heterogeneous Pd-catalyst $Ce_{0.20}Sn_{0.79}Pd_{0.01}O_{2-\delta}$

The used heterogeneous Pd-catalysts of formula $Ce_{0.20}Sn_{0.79}Pd_{0.01}O_{2-\delta}$ was synthesized using a modified solution combustion method, which was already reported by Baidya et al [4]. For the synthesis of 3 g catalyst, ammonium cerium(IV) nitrate (2.12 g), tin(II) oxalate (3.16 g), palladium(II) chloride (34 mg) glycine (3.35 g) were pestled in a mortar until a fine powder was achieved. HPLC-grade water (2 mL) was added and the mixture was sonicated for 30 min. After combustion in the oven for 1 h at 350 °C, the catalyst was pestled again and the resulting yellow powder was dried in the oven over night at 350 °C. The catalyst was obtained in quantitative yield and used as such for Suzuki-Miyaura cross-coupling reactions.

1.4 Design of Experiments

For the DoE analysis of Boc-deprotection and *N*-amidation in continuous flow, the software MODDE Pro (Version 12.1.0.5491, Copyright © Sartorius Stedim Data Analytics AB) was utilized. In both cases, we chose a full-factorial design with 2 quantitative multilevel factors (Boc-deprotection: *T* and *mol eq. HCl*, *N*-amidation: *Mol eq. succinic anhydride* and *mol eq. DIPEA*) and 2 replicates of the center point. As response factor, we set the conversion of compounds **17** and **18**, respectively. The corresponding experimental raw data used for DoE analysis is given in Table 5 (Boc-deprotection) and Table 6 (*N*-amidation).

Table 5: Experimental raw data for DoE analysis of Boc-deprotection in continuous flow.

Entry	T [°C]	Mol eq. HCl []	Conversion [%][a]
1	80	5	81.4
2	75	5	61.7
3	70	5	46.4
4	80	10	96.9
5	75	10	87.4
6	75	10	87.6
7	75	10	86.6
8	70	10	69.5
9	80	15	>99.9
10	75	15	97.6
11	70	15	87.8

[a] Conversion of **17** determined as mean value of measured conversion at τ= 3, 3.5, 4 (determined by HPLC)

Table 6: Experimental raw data for DoE analysis of *N*-amidation in continuous flow.

Entry	Mol eq. $Succ_2O$ []	Mol eq. DIPEA []	Conversion [%][a]
1	2.0	1.5	97.5
2	2.0	1.0	97.7
3	2.0	0.5	97.0
4	1.5	1.5	89.4
5	1.5	1.0	93.7
6	1.5	1.0	93.4
7	1.5	1.0	93.6
8	1.5	0.5	93.4
9	1.0	1.5	60.5
10	1.0	1.0	73.1
11	1.0	0.5	78.6

[a] Conversion of **18** determined as mean value of measured conversion at τ= 3, 3.5, 4 (determined by HPLC)

Regarding the DoE analysis of Boc-deprotection, first the replicate plot of the experimental data (A, Figure 13) showed low variability of the replicates. The corresponding histogram plot revealed approximate normal distribution of the experimental data and therefore, no data transformation was necessary. Furthermore, "*temperature*", "*mol eq. HCl*", "*mol eq. HCl*mol eq. HCl*" as well as "*temperature*mol eq. HCl*" were identified to be significant model terms (C, Figure 13). The statistical parameters of obtained model are given in Table 7 as well as visualized in the Fit plot (B, Figure 13). The performance indicators R^2 (0= no model, 1= perfect model) and Q^2 (>0.5) indicate a very useful model. Furthermore, the low variation of the replicates compared to the overall variability is reflected in the high value for the model reproducibility (>0.5). The validity of the model exhibits a relatively low value. However, very good models (Q^2>0.9) or models with extremely good replicates are prone to show low model validity due to the high sensitivity in the test. Furthermore, the normal probability plot (D, Figure 13) displays the absence of outliers and as the points approximately resemble a straight line, the residuals are likely to be normally distributed noise.

Concerning the DoE analysis of *N*-amidation, the replicate plot again revealed low variability of the replicates (A, Figure 14). Owing to the fact that the histogram plot indicated negative skewness, a negative logarithmic transformation of the data was performed. In the following, the model terms "*mol eq. succinic anhydride*", "*mol eq. DIPEA*", "*mol eq. DIPEA* mol eq. DIPEA*" and "*mol eq. succinic anhydride*mol eq. DIPEA*" were identified to have a significant influence on the response and were therefore included in the model (C, Figure 14). The statistical parameters describing the model quality are given in Table 7 and depicted in the Fit plot (B, Figure 14). Again, the relatively low model validity can be probably ascribed to the low replicate variability. Once more, the normal probability plot (D, Figure 14) suggests the residuals to be normally distributed noise.

Table 7: Statistical parameters of the DoE-models for Boc-deprotection and *N*-amidation.

Statistical parameter	Model Boc-deprotection	Model *N*-amidation
R^2	0.986526	0.991149
Q^2	0.941737	0.965226
Model validity	0.122941	0.10089
Reproducibility	0.998978	0.999386

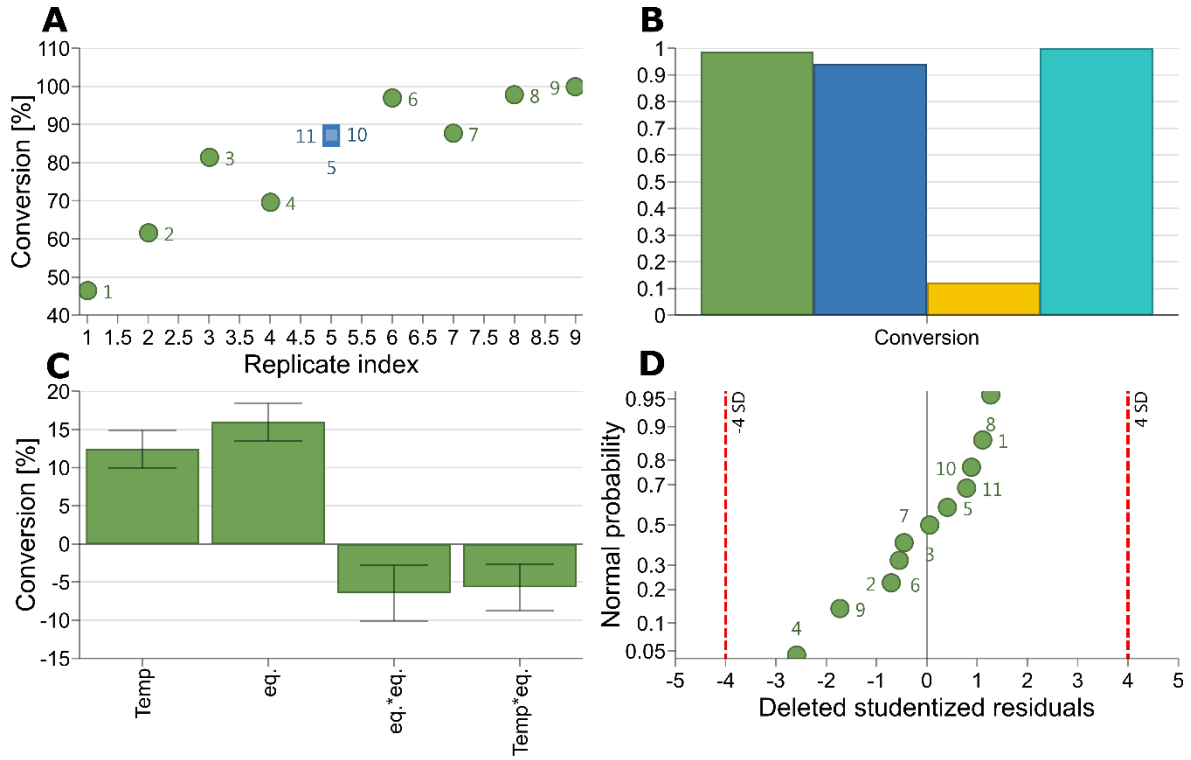

Figure 13: Overview plot of the Boc-deprotection model created with MODDE Pro (A: Replicate Plot, B: Summary of Fit Plot, C: Coefficient Plot, D: Residuals Normal Probability Plot).

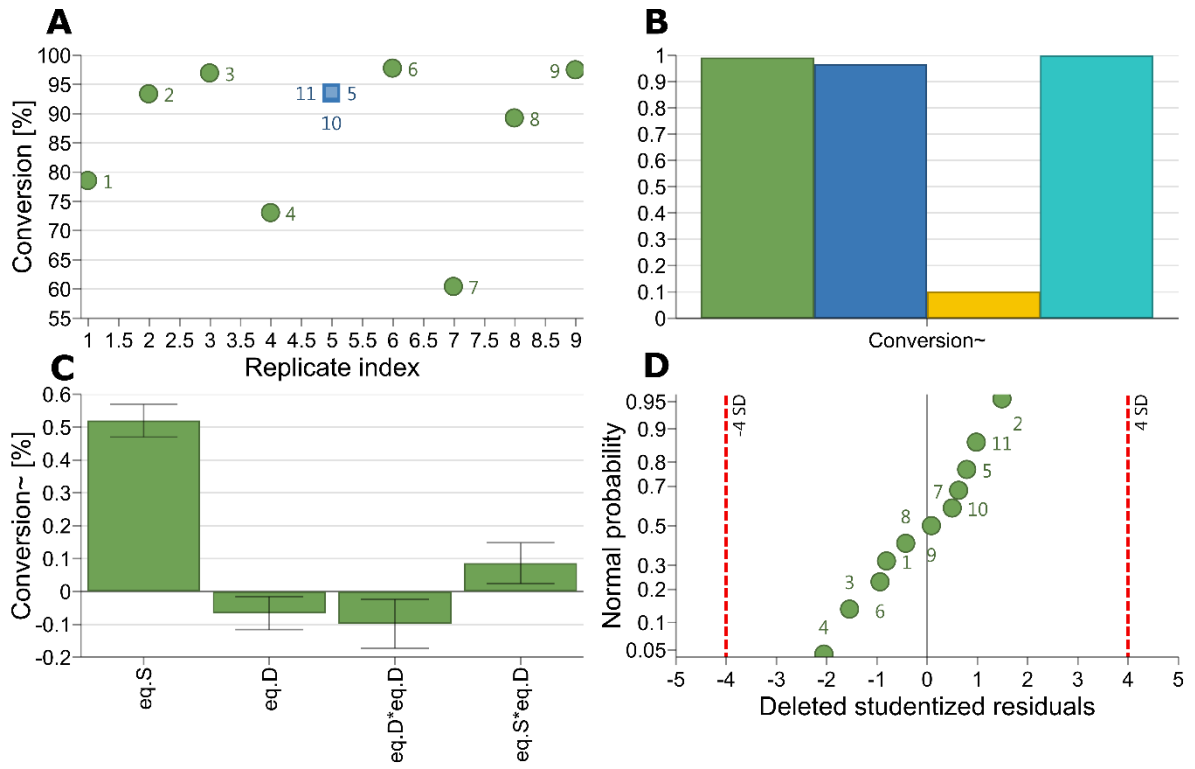

Figure 14: Overview plot of the *N*-amidation model created with MODDE Pro (A: Replicate Plot, B: Summary of Fit Plot, C: Coefficient Plot, D: Residuals Normal Probability Plot).

1.5 Multistep continuous setup for the synthesis of 16

The course of conversion of starting compound **13** as well as the yield of target molecule **16** over time using the three-step continuous setup is apparent from Figure 15.

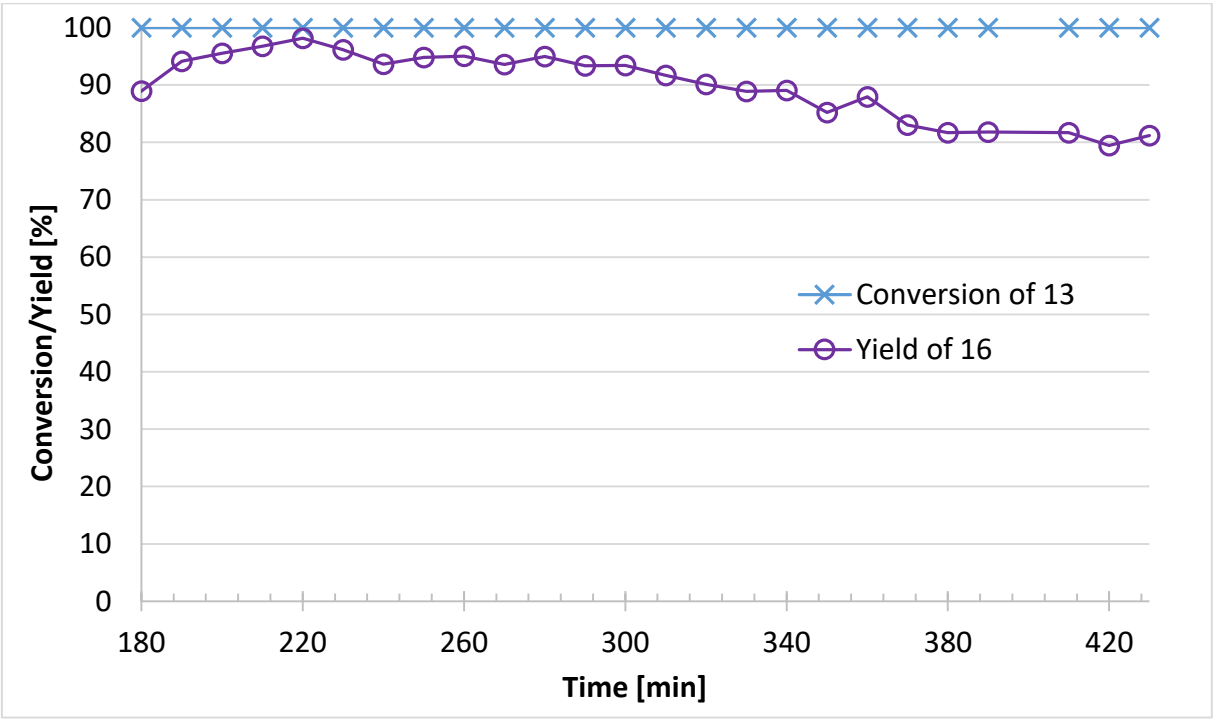

Figure 15: Conversion of **13** and yield of **16** utilizing the multistep setup for the synthesis of sacubitril precursor **16** in continuous flow (at t= 400 min: refill of syringe in syringe pump, no sample was taken).

1.6 References

1. Ksander GM, Ghai RD, deJesus R, Diefenbacher CG, Yuan A, Berry C, Sakane Y, Trapani A (1995) J Med Chem 38:1689-1700
2. Chai Y, Ullrich A, Kazmaier U, Muller R (2010) Bioactive pre-tubulysins and use thereof. PCT Int. Appl. WO 2010/034724 A1, Apr 1, 2010; (2010) Chem Abstr 166:485194
3. Wang Y, Chen F-E, Shi Y, Tian W-S (2016) Tetrahedron Lett 57:5928-5930
4. Baidya T, Gupta A, Deshpandey PA, Madras G, Hegde MS (2009) J Phys Chem C 113:4059-4068